

Tripodal Organic Cages with Unconventional CH \cdots O Interactions for Perchlorate Remediation in Water

Jayanta Samanta,^{1,3} Miao Tang,¹ Mingshi Zhang,¹ Russell P. Hughes,¹ Richard J. Staples,² Chenfeng Ke^{1*}

¹ Department of Chemistry, Dartmouth College, 41 College Street, Hanover, NH 03755, United States

² Department of Chemistry, Michigan State University, 578 S. Shaw Lane, East Lansing, MI 48824, United States

³ Department of Chemistry, College of Engineering and Technology, SRM Institute of Science and Technology, Kattankulathur 603203, India

Email: Chenfeng.Ke@dartmouth.edu

ABSTRACT: Perchlorate anions used in industry are harmful pollutants in groundwater. Therefore, selectively binding perchlorate provides solutions for environmental remediation. Here, we synthesized a series of tripodal organic cages with highly pre-organized C_{sp³}–H bonds that exhibit selectively binding to perchlorate in organic solvents and water. These cages demonstrated binding affinities to perchlorate of 10^{5–6} M^{–1} at room temperature, along with high selectivity over competing anions such as iodide and nitrate. Through single crystal structure analysis and density functional theory calculations, we identified unconventional C_{sp³}–H \cdots O interactions as the primary driving force for perchlorate binding. Additionally, we successfully incorporated this cage into a 3D-printable polymer network, showcasing its efficacy in removing perchlorate from water.

Perchlorates (ClO₄[–]) are widely used in rocket propellants, explosives, oxidizing agents, and other industrial purposes.^{1,2} These highly soluble but toxic compounds enter the water systems and the food chain, posing threats to human health and environmental safety.³ Current methods for removing perchlorate, such as anion exchange,⁴ lack sufficient selectivity in separating it from competing anions.⁵ Therefore, there is a need to develop perchlorate-specific binding receptors with good affinity and selectivity in water.⁶ These receptors, when integrated into polymer networks,^{7–9} will facilitate the selective removal of perchlorate.

Early designs of receptors utilize NH or OH hydrogen bonding for ClO₄[–] binding in organic solvents.¹⁰ However, when applied to aqueous environments, these designs suffered from drastically reduced affinity and selectivity due to water's competition for hydrogen bonding sites.^{11,12} Recent advancements have explored non-classical C_{sp²}–H^{13,14} and C_{sp³}–H¹⁵ hydrogen bonding motifs and halogen bonding moieties¹⁶ for anion binding in water.^{17,18} Some high affinitive anion binding was achieved through pre-organized hydrogen bonding arrays and hydrophobic effect.^{19–22} Examples include a high-affinity chloride-binding cage reported by Flood *et al.* with polarized C_{sp²}–H donors,²³ and a water-soluble bambus[6]uril reported by Sinselar *et al.* that displays a strong affinity for ClO₄[–] through serendipitously discovered C_{sp³}–H bonding interactions.^{24,25} These discoveries inspired us to intentionally bring C_{sp³}–H bonds to design anion-binding receptors.

Herein, we designed rigid tripodal cages featuring piperazine-based pillars with highly pre-organized C_{sp³}–H bonds, which selectively bind ClO₄[–] anion in organic solvent and water

(Figure 1). X-ray diffraction and binding studies of the inclusion complexes provided an unambiguous understanding of the unconventional C_{sp³}–H \cdots O interactions. Furthermore, the cage was utilized as a 3D-printing material to create hydrogels capable of removing ClO₄[–] anions from water.

Tripodal cage **C1** was synthesized in four steps (Scheme S1). First, **S1** was synthesized by reacting *Boc*-piperazine with benzenetricarbonyl-trichloride, followed by *Boc*-deprotection. The reaction of **S1** with cyanuric chloride yielded **S2**. Macrocyclization of **S1** and **S2** under high dilution afforded **C1**. When dioxane was introduced as a co-solvent, **C1** was obtained in 55% yield without chromatography purifications. Substituting the remaining chloride in **C1** allows easy access to **C1_{allyl}**, **C1_{N-Boc}**, **C1NH₃Cl**, and **C1_{AM}** in good yields (Figure 1b).

C1_{allyl} has good solubility in chlorinated solvents, 1,4-dioxane, and DMSO. Single crystals of **C1_{allyl}** were obtained by diffusing hexane into a dioxane solution of **C1_{allyl}**. In the single-crystal X-ray diffraction (SCXRD) analysis, the top and bottom benzene moieties of **C1_{allyl}** are 11.0 Å apart, and the piperazine moieties adopt chair conformations with equatorial C–H bonds oriented toward the center of the cavity (Figure 2a). **C1_{allyl}** was filled by one dioxane with multiple C–H \cdots O interactions (Figure 2a), suggesting dioxane as a template for the macrocyclization as confirmed earlier. ¹H NMR titration of dioxane to **C1_{allyl}** in CDCl₃ at 298 K showed no noticeable binding, possibly due to CDCl₃ acting as a competing guest (Figure S36).

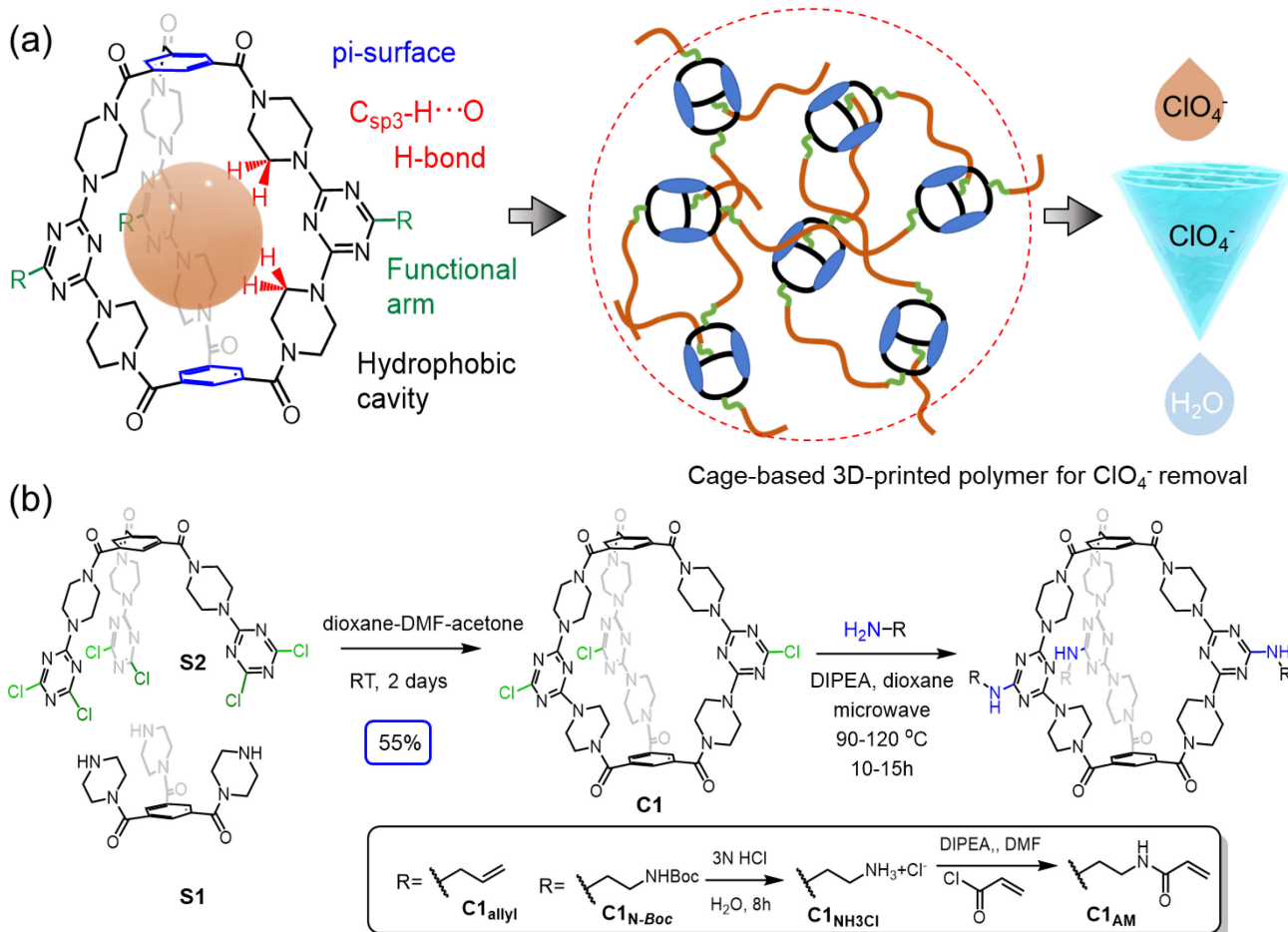


Figure 1. (a) Design of tripodal cages and their 3D-printed polymer networks for perchlorate recognition and remediation. (b) Synthesis of **C1**-based tripodal cages.

Unlike alkyl-piperazines,²⁶ the acyl-piperazine moieties of **C1_{allyl}** exhibit limited rotational freedom in solution, evident in the ^1H NMR spectra in CDCl_3 and $\text{DMSO}-d_6$ (Figure 2b). Four sets of non-equivalent protons connected to C_b , C_c , C_d , and C_e were assigned through 2D NMR experiments (Figures S10-S12, S16-S19). This phenomenon is similar to acyl-piperazine derivatives,²⁷ in which the chair flipping remained, but the $\text{C}-\text{N}$ bond rotation is limited due to the enol-iminium resonance structure. The crystal structure of **C1_{allyl}** confirms the partial double bond nature of the $\text{O}=\text{C}-\text{N}$ bonds with short $\text{C}-\text{N}$ bond lengths (1.34–1.36 Å) and longer $\text{C}=\text{O}$ bond lengths (1.22–1.24 Å, Figure S84). The *anti*- H_b and *anti*- H_c to the carbonyl oxygen atom point toward the cavity, providing a highly pre-organized binding site.

When **C1_{allyl}** was mixed with 10 equivalents of tetrabutylammonium (TBA) salts in CDCl_3 , notable shifts were observed for the aromatic proton H_a and piperazine protons $\text{H}_{b/c/d/e}$ in the ^1H NMR spectra (Figure S37), indicating fast associations at the NMR time scale. In the ^1H NMR titration of **C1_{allyl}** and TBAClO_4 in CDCl_3 , the H_a and H_b protons shifted upfield while H_c protons shifted downfield significantly (Figure 3a). The binding affinities between **C1_{allyl}** and these anions were fitted using a 1:1 binding model as K_a : $\text{Cl}^- < \text{Br}^- < \text{NO}_3^- < \text{I}^- < \text{BF}_4^- < \text{PF}_6^- < \text{ClO}_4^-$ (Table 1), which align with the Hofmeister series.^{21,22} The binding affinity between **C1_{allyl}** and ClO_4^- reached $7.5 \times 10^5 \text{ M}^{-1}$. Notably, the $\text{ClO}_4^-/\text{I}^-$ selectivity of **C1_{allyl}** is calculated as 300, much larger than bambus[6]uril (~ 1), even

though it has a lower affinity.²⁸ In comparison, an analogous open-formed **T1** (Scheme S5) showed no appreciable binding towards anions (Figure S69), highlighting the benefit of the pre-organized cavity.

Increasing the solvent polarity to $\text{DMSO}-d_6$ decreased the binding affinities towards all anions. In $\text{DMSO}-d_6$, **C1_{allyl}** showed binding affinities for I^- and ClO_4^- as 25 and 75 M^{-1} , respectively (Table 1). When 10% D_2O was added to $\text{DMSO}-d_6$, the binding affinities increased to 33 and 171 M^{-1} , respectively, with an improved $\text{ClO}_4^-/\text{I}^-$ selectivity. These results suggest that the hydrophobic effect effectively promotes anion binding. The high affinitive anion binding in CDCl_3 and low affinitive binding in $\text{DMSO}-d_6$ resemble the behavior of many hydrogen-bond-based receptors.^{29,30} Given that the solvophobic effect of DMSO is not the primary factor, we speculate that the anion-**C1_{allyl}** interaction may contain unconventional hydrogen bonding interactions.

To verify this, $\text{TBAClO}_4 \cdot \text{C1}_{\text{allyl}}$ crystals were obtained for SCXRD analysis. In the solid state, one ClO_4^- anion was included in the cavity of **C1_{allyl}**, and another ClO_4^- anion bound to the cage's aperture (Figures 3b, S88-S91).

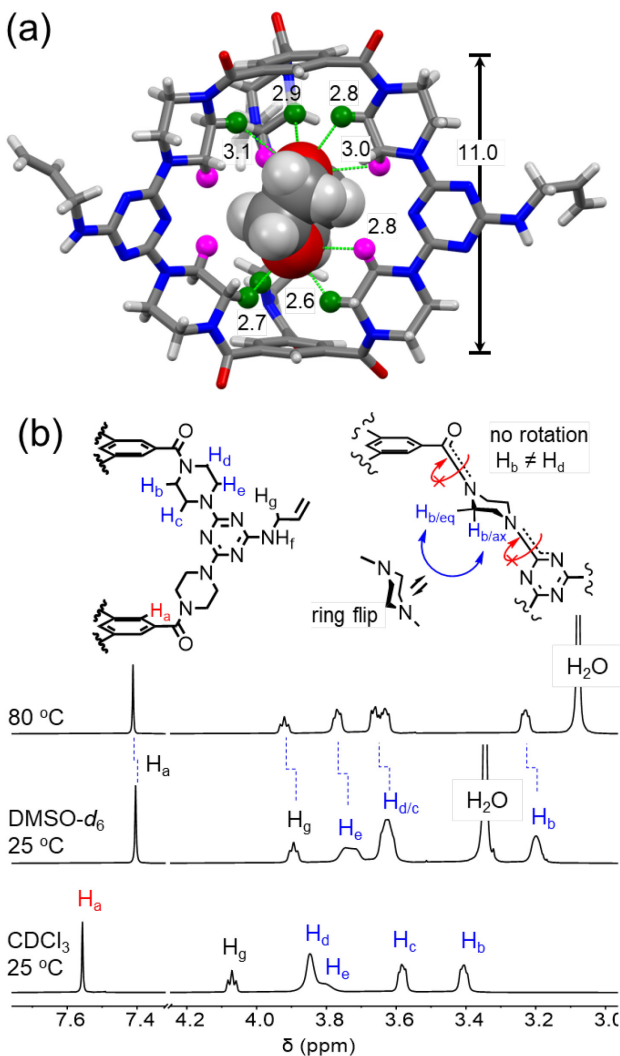


Figure 2. (a) X-ray structure of **C1_{allyl}** with a 1,4-dioxane. Equatorial C_{sp³}-H protons were highlighted in green and purple colors. The distances of the C_{sp³}-H...O contacts are in Å. (b) ¹H NMR spectra of **C1_{allyl}** in different solvents and temperatures.

Table 1. Binding affinity (K_a) and thermodynamic parameters (ΔH , $T\Delta S$, and ΔG) of **C1_{allyl}** and **C1_{NH3Cl}** with anions (298 K).

anion	C1_{allyl}		C1_{NH3Cl}			
	CDCl ₃ *	DMSO-d ₆ * [10% D ₂ O]	$K_a^{\#}$ (M ⁻¹)	ΔH (kJ/mol)	$T\Delta S$ (kJ/mol)	ΔG (kJ/mol)
	K_a (M ⁻¹)	K_a (M ⁻¹)				
F ⁻	32 ± 1	< 5	< 5	n.d.	n.d.	n.d.
Cl ⁻	9 ± 2	< 5	51 ± 0.9	-27.2 ± 0.3	17.3 ± 1.0	-9.9 ± 0.1
Br ⁻	26 ± 2	< 5	308 ± 45	-17.1 ± 2.1	-2.8 ± 2.1	-14.3 ± 0.1
I ⁻	(2.4 ± 0.1) × 10 ³	25 ± 3 [33 ± 2]	(1.8 ± 0.4) × 10 ⁴	-30.5 ± 2.0	-6.3 ± 1.4	-24.3 ± 0.6
NO ₃ ⁻	(1.0 ± 0.2) × 10 ³	< 5	731 ± 46	-16.0 ± 0.3	0.4 ± 0.3	-16.4 ± 0.1
BF ₄ ⁻	(4.5 ± 0.9) × 10 ⁴	18 ± 1	(6.6 ± 0.3) × 10 ⁴	-35.8 ± 1.5	-8.5 ± 1.0	-27.4 ± 0.5
PF ₆ ⁻	(1.4 ± 0.1) × 10 ⁵	66 ± 1	(7.9 ± 0.8) × 10 ⁵	-44.9 ± 2.4	-11.3 ± 1.6	-33.7 ± 1.2
ClO ₄ ⁻	(7.5 ± 0.2) × 10 ⁵	75 ± 3 [171 ± 4]	(2.5 ± 0.1) × 10 ⁵	-42.3 ± 0.3	-11.0 ± 0.2	-31.3 ± 0.4
	in 1 mM Na ₂ SO ₄ solution		(2.4 ± 0.1) × 10 ⁵	-36.0 ± 0.3	-5.5 ± 0.2	-30.5 ± 0.3
	in 0.5 M		(1.8 ± 0.1) × 10 ⁴	-16.2 ± 0.1	8.0 ± 0.1	-24.2 ± 0.1
	and 1 M NaCl solutions		(1.4 ± 0.2) × 10 ⁴	-14.8 ± 0.9	8.7 ± 1.3	-23.5 ± 0.4

*TBA salts used for ¹H NMR titrations, [#]NaCl/Br/NO₃/BF₄, KI/ClO₄/PF₆ used for ITC. n.d. for not determined.

The included ClO₄⁻ anion fits within the cavity with multiple short C-H...O distances ranging from 2.5 to 3.1 Å. The ClO₄⁻•C1_{allyl} complex was simulated using density functional theory (DFT) with B3LYP-D3/6-31G** and subjected to an energy decomposition analysis.³¹ The total bonding energy in vacuo ($E_{\text{int}} = -229.5$ kJ/mol) between C1_{allyl} and ClO₄⁻ comprises various components, which allow for differentiation between attractive donor-acceptor ($E_{\text{orb}} = -97.1$ kJ/mol), electrostatic ($E_{\text{stat}} = -166.9$ kJ/mol), dispersion ($E_{\text{disp}} = -89.7$ kJ/mol), and repulsive interactions ($E_{\text{Pauli}} = +124.5$ kJ/mol). Notably, E_{orb} is significant and consists of many small interactions between the lone pair of oxygens and piperazine's C-H σ* orbitals (Figure 3c). This analysis suggests that there are multivalent weak hydrogen bonds in the complex, which are stabilized further through dispersion and electrostatic attractions. Although each C_{sp³}-H...O hydrogen bonding is weak, the multivalency and cooperativity in this highly pre-organized cage enabled good affinity binding of ClO₄⁻.

The hydrophobic binding site³² and the multivalent C_{sp³}-H...O interactions indicate that the binding for ClO₄⁻ could be further enhanced in water. Therefore, we synthesized a water-soluble C1_{NH3Cl} (Figure 1b) and investigated its binding with different anions using isothermal titration calorimetry (ITC, Figure 3d and Table 1). At 25 °C, C1_{NH3Cl} demonstrated a good affinity for ClO₄⁻ of 2.5×10^5 M⁻¹ and a high ClO₄⁻/I⁻ selectivity of 14 in water, while the binding with SO₄²⁻ is very weak (< 5 M⁻¹, Figure S68). Although the ion-ion interactions between the cationic ethylammonium arms and ClO₄⁻ may contribute to the overall binding, we conducted ITC experiments with 0.5 and 1 M NaCl to shield these Coulombic interactions,^{21, 22} despite increasing the solvent's dielectric constant and introducing a competing Cl⁻ anion. Remarkably, C1_{NH3Cl} remained good affinity binding for ClO₄⁻ in these highly concentrated NaCl solutions with K_a of $1.4-1.8 \times 10^4$ M⁻¹ (Table 1). Notably, the enthalpy contribution remains significant to the overall binding, providing additional evidence for the nature of C_{sp³}-H...O interactions as weak hydrogen bonds.

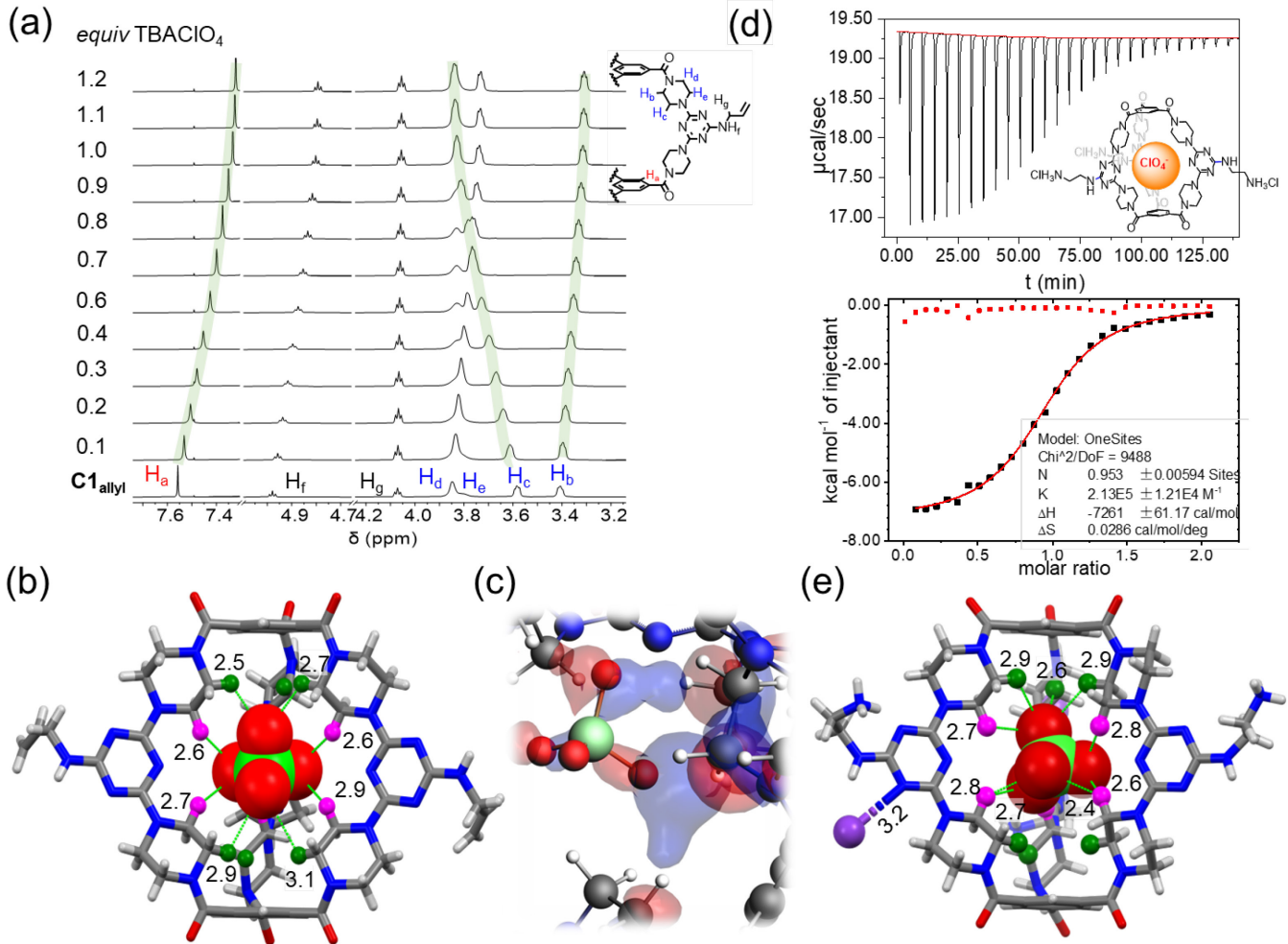


Figure 3. (a) ¹H NMR titration of C1_{allyl} (1 mM) with the addition of TBAClO₄ in CDCl₃ at 298 K. (b) Single-crystal structure of TBAClO₄•C1_{allyl} and the highlighted C_{sp}³-H...O contacts in Å. (c) A snapshot of the interactions between lone pairs of oxygens and σ^* orbitals of C-H bonds provided by DFT calculation. (d) The ITC experiment of adding KClO₄ to an aqueous solution of C1_{NH3Cl} (0.1 mM). The data were fitted to a 1:1 binding model. (e) Single-crystal structure of KClO₄•C1_{NH3Cl} and the highlighted C_{sp}³-H...O contacts in Å.

Furthermore, the single crystal structure of KClO₄•C1_{NH3Cl} showed a similar conformation to the TBAClO₄•C1_{allyl} complex (Figure S94-S95), with short C-H...O distances ranging from 2.4 to 2.9 Å (Figure 3e), compared to the combined van der Waals' radii of 2.72 Å (H + O).³³ The ethylammoniums of C1_{NH3Cl} are not flexible enough to fold backward for intramolecular ion-ion interactions, confirming that ion-ion interactions are not the key driving force for the complexation.

We incorporated C1 as an active perchlorate removal moiety into a polymer network to investigate its suitability for ClO₄⁻ remediation in water. A C1_{AM} crosslinker was synthesized from C1_{NH3Cl} for the copolymerization with *N,N*-dimethylacrylamide (DMA, 100 equiv., Figure 4a). In the presence of 2,2-dimethoxy-2-phenylacetophenone (DMPA) and a 3D-printing template Pluronic F127, a hydrogel with good shear-thinning and self-healing properties (Figure S107) was formed via our hierarchical co-assembly direct-ink-writing method.^{34, 35} This

hydrogel was 3D-printed into a cone shape paired with a glass funnel to set up a purification stand. After 3D-printing, it was photo-polymerized to form a crosslinked 3DP-C1_{AM}-net (Figure 4b).

When 3DP-C1_{AM}-net was immersed in an aqueous solution of KClO₄ (0.125 mM, 17.3 ppm),³⁶ the conductance of the solution rapidly decreased over time (Figure 4c). After 2 h, the residual ClO₄⁻ concentration reached 0.025 mM and after 20 h, it decreased to 0.017 mM. In comparison, a control AM-net synthesized using pentaerythritol triacrylate and DMA (Scheme S7) showed negligible ClO₄⁻ removal capability. We assessed the reusability of the 3DP-C1_{AM}-net by subjecting it to five cycles of ClO₄⁻ removal and regeneration (Figure 4d, S116). The 3DP-C1_{AM}-net hydrogel showed only a marginal decrease in performance, indicating its robustness for ClO₄⁻ remediation.

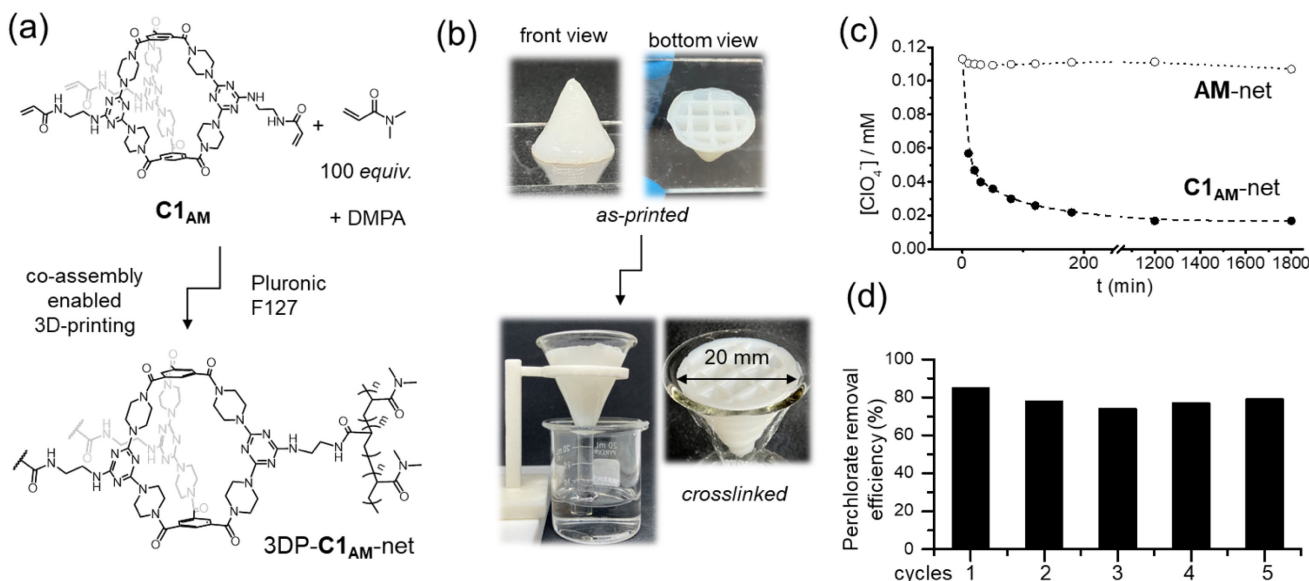


Figure 4. (a) Synthesis of crosslinked 3D-printed 3DP-**C1_{AM}**-net using **C1_{AM}**. (b) 3D-printed cone-shaped funnels before (top) and after crosslinking (bottom, with its perchlorate removal setup) using an F127 hydrogel (40 w/v%) with **C1_{AM}** (20 mM), DMA (1.8 M), and DMPA (78 mM). (c) Time-dependent conductance of KClO₄ solution (0.125 mM) in the presence of crosslinked **C1_{AM}**-net and **AM**-net. (d) Reusability of the crosslinked **C1_{AM}**-net for ClO₄⁻ removal.

In summary, our investigation of rigid tripodal cages featuring piperazine pillars leads to the understanding of unconventional C_{sp³}-H^{•••}O hydrogen bonding interactions with perchlorate. X-ray diffraction analysis confirmed the short contacts between the C_{sp³}-H bonds and ClO₄⁻. Titration studies provided quantitative analysis of the binding affinities and thermodynamic parameters of the complexes. DFT calculations reveal the C_{sp³}-H^{•••}O interaction originates from the interaction between the lone pairs of oxygen atoms and the piperazine C-H σ* orbitals. These cages exhibited good affinity and selectivity for perchlorate in organic solvents and water. We also demonstrated their application as a 3D printing material, creating a hydrogel capable of efficiently and repeatedly removing ClO₄⁻ anions from water, presenting a promising pathway for incorporating molecular designs into useful polymer networks for clean water.

ASSOCIATED CONTENT

Supporting Information.

Synthesis and characterization of the compounds, NMR and ITC titration experiments, X-ray crystallographic analyses, DFT calculations, rheological data, 3D printing of polymers and ClO₄⁻ removal details are available free of charge (PDF).

Accession Codes

CCDC 2244494, 2244495, 2247551, contains the supplementary crystallographic data for this paper. These data can be obtained free of charge via www.ccdc.cam.ac.uk/data_request/cif, or by emailing data_request@ccdc.cam.ac.uk, or by contacting The Cambridge Crystallographic Data Centre, 12 Union Road, Cambridge CB2 1EZ, UK; fax: +44 1223 336033.

AUTHOR INFORMATION

Corresponding Author

* Chenfeng Ke, Department of Chemistry, Dartmouth College, 41 College Street, Hanover, NH 03755, United States
Email: Chenfeng.Ke@dartmouth.edu

Authors

Jayanta Samanta, Department of Chemistry, Dartmouth College, 41 College Street, Hanover, NH 03755, United States; Department of Chemistry, College of Engineering and Technology, SRM Institute of Science and Technology, Kattankulathur 603203, India

Miao Tang, Department of Chemistry, Dartmouth College, 41 College Street, Hanover, NH 03755, United States

Mingshi Zhang, Department of Chemistry, Dartmouth College, 41 College Street, Hanover, NH 03755, United States

Russell Hughes, Department of Chemistry, Dartmouth College, 41 College Street, Hanover, NH 03755, United States

Richard Staples, Department of Chemistry, Michigan State University, 578 S. Shaw Lane, East Lansing, MI 48824, United States

Notes

The authors declare no competing financial interest.

ACKNOWLEDGMENT

This work is supported by the National Science Foundation CAREER award (DMR-1844920), the Arnold and Mabel Beckman Foundation BYI program, and Dartmouth Scholarly Innovation and Advance Award. The MRI program provided funding for the Single Crystal X-ray diffractometer at MSU by the National Science Foundation under Grant No. 1919565. We thank Professor Dean Wilcox at Dartmouth College for the access to the ITC instrument.

REFERENCES

- Jacobs, P. W. M.; Whitehead, H. M. Decomposition and combustion of ammonium perchlorate. *Chem. Rev.* **1969**, *69*, 551-590. DOI: 10.1021/cr60260a005
- Trache, D.; Klapotke, T. M.; Maiz, L.; Abd-Elghany, M.; DeLuca, L. T. Recent advances in new oxidizers for solid rocket propulsion. *Green Chem.* **2017**, *19*, 4711-4736. DOI: 10.1039/c7gc01928a
- Srinivasan, A.; Viraraghavan, T. Perchlorate: Health effects and technologies for its removal from water resources. *Int. J. Env. Res. Pub. He.* **2009**, *6*, 1418-1442. DOI: 10.3390/ijerph6041418
- Xie, Y. H.; Ren, L. L.; Zhu, X. Q.; Gou, X.; Chen, S. Y. Physical and chemical treatments for removal of perchlorate from water-A review. *Process Saf. Environ.* **2018**, *116*, 180-198. DOI: 10.1016/j.psep.2018.02.009
- Song, W.; Gao, B. Y.; Guo, Y.; Xu, X.; Yue, Q. Y.; Ren, Z. F. Effective adsorption/desorption of perchlorate from water using corn stalk based modified magnetic biopolymer ion exchange resin. *Micropor. Mesopor. Mat.* **2017**, *252*, 59-68. DOI: 10.1016/j.micromeso.2017.06.019
- Kubik, S. Anion recognition in water. *Chem. Soc. Rev.* **2010**, *39*, 3648-3663. DOI: 10.1039/b926166b
- Ji, X. F.; Wu, R. T.; Long, L. L.; Guo, C. X.; Khashab, N. M.; Huang, F. H.; Sessler, J. L. Physical removal of anions from aqueous media by means of a macrocycle-containing polymeric network. *J. Am. Chem. Soc.* **2018**, *140*, 2777-2780. DOI: 10.1021/jacs.7b13656
- Wang, H.; Ji, X. F.; Ahmed, M.; Huang, F. H.; Sessler, J. L. Hydrogels for anion removal from water. *J. Mater. Chem. A* **2019**, *7*, 1394-1403. DOI: 10.1039/c8ta10286d
- Bak, K. M.; Patrick, S. C.; Li, X.; Beer, P. D.; Davis, J. J. Engineered binding microenvironments in halogen bonding polymers for enhanced anion sensing. *Angew. Chem. Int. Ed.* **2023**, *62*, e202300867. DOI: 10.1002/anie.202300867
- Yang, L. Z.; Li, Y.; Jiang, L.; Feng, X. L.; Lu, T. B. Size and temperature dependent encapsulation of tetrahedral anions by a protonated cryptand host. *Crystengcomm.* **2009**, *11*, 2375-2380. DOI: 10.1039/b904838c
- Edwards, S. J.; Valkenier, H.; Busschaert, N.; Gale, P. A.; Davis, A. P. High-affinity anion binding by steroid squaramide receptors. *Angew. Chem. Int. Edit.* **2015**, *54*, 4592-4596. DOI: 10.1002/anie.201411805
- Li, H. Y.; Valkenier, H.; Judd, L. W.; Brotherhood, P. R.; Hussain, S.; Cooper, J. A.; Jurcek, O.; Sparkes, H. A.; Sheppard, D. N.; Davis, A. P. Efficient, non-toxic anion transport by synthetic carriers in cells and epithelia. *Nat. Chem.* **2016**, *8*, 24-32. DOI: 10.1038/Nchem.2384
- Lee, S.; Chen, C. H.; Flood, A. H. A pentagonal cyanostar macrocycle with cyanostilbene CH donors binds anions and forms dialkylphosphate [3]rotaxanes. *Nat. Chem.* **2013**, *5*, 704-710. DOI: 10.1038/Nchem.1668
- Eytel, L. M.; Faragher, H. A.; Haley, M. M.; Johnson, D. W. The road to aryl CH···anion binding was paved with good intentions: fundamental studies, host design, and historical perspectives in CH hydrogen bonding. *Chem. Commun.* **2019**, *55*, 5195-5206, 10.1039/C9CC01460H. DOI: 10.1039/C9CC01460H
- Shyshov, O.; Siewerth, K. A.; von Delius, M. Evidence for anion-binding of all-cis hexafluorocyclohexane in solution and solid state. *Chem. Commun.* **2018**, *54*, 4353-4355. DOI: 10.1039/C8CC01797B
- Cavallo, G.; Metrangolo, P.; Pilati, T.; Resnati, G.; Sansotera, M.; Terraneo, G. Halogen bonding: a general route in anion recognition and coordination. *Chem. Soc. Rev.* **2010**, *39*, 3772-3783. DOI: 10.1039/B926232F
- Langton, M. J.; Robinson, S. W.; Marques, I.; Felix, V.; Beer, P. D. Halogen bonding in water results in enhanced anion recognition in acyclic and rotaxane hosts. *Nat. Chem.* **2014**, *6*, 1039-1043. DOI: 10.1038/Nchem.2111
- Chen, L. J.; Berry, S. N.; Wu, X.; Howe, E. N. W.; Gale, P. A. Advances in anion receptor chemistry. *Chem.* **2020**, *6*, 61-141. DOI: 10.1016/j.chempr.2019.12.002
- Macreadie, L. K.; Gilchrist, A. M.; McNaughton, D. A.; Ryder, W. G.; Fares, M.; Gale, P. A. Progress in anion receptor chemistry. *Chem.* **2022**, *8*, 46-118. DOI: 10.1016/j.chempr.2021.10.029
- Sarkar, S.; Ballester, P.; Spektor, M.; Kataev, E. A. Micromolar affinity and higher: synthetic host-guest complexes with high stabilities. *Angew. Chem. Int. Edit.* **2023**, *e202214705*. DOI: 10.1002/anie.202214705.
- Gibb, C. L. D.; Gibb, B. C. Anion binding to hydrophobic concavity is central to the salting-in effects of Hofmeister chaotropes. *J. Am. Chem. Soc.* **2011**, *133*, 7344-7347. DOI: 10.1021/ja203208n
- Carnegie, R. S.; Gibb, C. L. D.; Gibb, B. C. Anion complexation and the Hofmeister effect. *Angew. Chem. Int. Edit.* **2014**, *53*, 11498-11500. DOI: 10.1002/anie.201405796
- Liu, Y.; Zhao, W.; Chen, C.-H.; Flood, A. H. Chloride capture using a C-H hydrogen-bonding cage. *Science* **2019**, *365*, 159-161. DOI: 10.1126/science.aaw5145
- Svec, J.; Dusek, M.; Fejfarova, K.; Stacko, P.; Klán, P.; Kaifer, A. E.; Li, W.; Hudeckova, E.; Sindelar, V. Anion-free bambus [6]uril and its supramolecular properties. *Chem. Eur. J.* **2011**, *17*, 5605-5612. DOI: 10.1002/chem.201003683
- Yawer, M. A.; Havel, V.; Sindelar, V. A bambusuril macrocycle that binds anions in water with high affinity and selectivity. *Angew. Chem. Int. Edit.* **2015**, *54*, 276-279. DOI: 10.1002/anie.201409895
- Lemaster, C. B.; Lemaster, C. L.; Suarez, C.; Tafazzoli, M.; True, N. S. Pressure-dependent and temperature-dependent proton NMR studies of N,N-dimethylpiperazine ring inversion in the gas-phase. *J. Phys. Chem.* **1989**, *93*, 3993-3996. DOI: 10.1021/j100347a026
- Wodtke, R.; Steinberg, J.; Köckerling, M.; Löser, R.; Mamat, C. NMR-based investigations of acyl-functionalized piperazines concerning their conformational behavior in solution. *RSC Adv.* **2018**, *8*, 40921-40933.
- Havel, V.; Sindelar, V. Anion binding inside a bambus[6]uril macrocycle in chloroform. *Chempluschem* **2015**, *80*, 1601-1606. DOI: 10.1002/cplu.201500345
- Lauer, J. C.; Bhat, A. S.; Barwig, C.; Fritz, N.; Kirschbaum, T.; Rominger, F.; Mastalerz, M. [2+3] Amide cages by oxidation of [2+3] imine cages - revisiting molecular hosts for highly efficient nitrate binding. *Chem. Eur. J.* **2022**, *28*, e20220152710. DOI: 10.1002/chem.202201527
- Qiao, B.; Anderson, J. R.; Pink, M.; Flood, A. H.; Size-matched recognition of large anions by cyanostar macrocycles is saved when solvent-bias is avoided. *Chem. Commun.* **2016**, *52*, 8683. DOI: 10.1039/c6cc03463b
- Sengupta, A.; Liu, Y.; Flood, A. H.; Raghavachari, K. Anion-binding macrocycles operate beyond the electrostatic regime: interaction distances matter. *Chem. Eur. J.* **2018**, *24*, 14409-14417. DOI: 10.1002/chem.201802657
- Sokkalingam, P.; Shrberg, J.; Rick, S. W.; Gibb, B. C. Binding hydrated anions with hydrophobic pockets. *J. Am. Chem. Soc.* **2016**, *138*, 48-51. DOI: 10.1021/jacs.5b10937
- Alvarez, S. A cartography of the van der Waals territories. *Dalton Trans.* **2013**, *42*, 8617. DOI: 10.1039/c3dt50599e
- Li, L. Y.; Zhang, P. F.; Zhang, Z. Y.; Lin, Q. M.; Wu, Y. Y.; Cheng, A.; Lin, Y. X.; Thompson, C. M.; Smaldone, R. A.; Ke, C. Hierarchical co-assembly enhanced direct ink writing. *Angew. Chem. Int. Edit.* **2018**, *57*, 5105-5109. DOI: 10.1002/anie.201800593
- Tang, M.; Zhong, Z.; Ke, C. Advanced supramolecular design for direct ink writing of soft materials. *Chem. Soc. Rev.* **2023**, *52*, 1614-1649. DOI: 10.1039/d2cs01011a
- Kosaka, K.; Asami, M.; Matsuoka, Y.; Kamoshita, M.; Kunikane, S. Occurrence of perchlorate in drinking water sources of metropolitan area in Japan. *Water Research*, **2007**, *41*, 3474 - 3482. DOI: 10.1016/j.watres.2007.05.011

Table of Contents

